NASA TECHNICAL MEMORANDUM

NASA TM X-62,225

NASA TM X-62,225

MIE SCATTERING OF THE INTERPLANETARY MAGNETIC FIELD BY THE WHOLE MOON

C. P. Sonett and D. S. Colburn

Ames Research Center
Moffett Field, Calif. 94035

January 1973

MIE SCATTERING OF THE INTERPLANETARY MAGNETIC FIELD BY THE WHOLE MOON

by

C. P. Sonett and D. S. Colburn
NASA Ames Research Center
Moffett Field, California 94035

ABSTRACT

It is known from the Apollo magnetometer experiments that significant electromagnetic induction takes place in the lunar interior. This induction is excited by fluctuations of the interplanetary magnetic field and is detected by the induced fields on the surface of the Moon. This paper reviews these results briefly and discusses the formal properties of the theory. It is shown that the mathematical treatment parallels that for classical electromagnetic scattering. Further the wavelength spectrum of the fluctuations of the interplanetary magnetic field include scales consistent with the radius of the Moon. The consequence is that the Moon is excited in several modes. Quadrupole and possibly octupole magnetic multipoles are found in the data. The electric type radiation corresponding to transverse magnetic (TM) excitation appears suppressed and so far below the detection threshold of the magnetometers, but electric multipoles should be present as well. If so they would tend to be restricted to the outer layers of the Moon.

INTRODUCTION

The purpose of this paper is to demonstrate the formal similarity between classical Mie scattering as known in optical phenomena and electromagnetic induction in the Moon caused by fluctuations of the interplanetary magnetic field. It is by now well known that the interplanetary magnetic field contains a continuum of disturbances which are seen by the Moon as time dependent variations in the direction and strength of the magnetic field (Sonett, et al., 1971). In turn these fluctuations result in the flow of eddy currents in the lunar interior whose magnetic field is detected on the surface of the Moon by comparison of records taken there using the Apollo surface magnetometers and the free stream solar wind field simultaneously monitored by lunar satellite Explorer 35 (Sonett, et al., 1972). From the concurrent Fourier spectra of the surface and solar wind magnetic fields the internal bulk electrical conductivity profile of the Moon can be determined using the classical equations of electromagnetic scattering.

The actual theory of scattering as is known for optical wave lengths and for vacuum conditions must be appropriately modified for the boundary conditions which exist at the contact between the Moon and solar wind. However the general formalism remains intact and we shall show later that the wavelength regime found in the solar wind which is responsible for the induction in the Moon is identifyable with magnetic multipole radiation including at least quadrupole and octupole terms. Proof of the effect of the solar wind in modifying the boundary conditions comes from observation that the lunar induction signal rises to values of 3-4 at the peak frequency, some 6-8

times that for vacuum induction. The increase is due to the dynamic pressure of the solar wind which forces the induced magnetic field lines back under the surface of the Moon. Skin depth arguments show that the confinement of the field varies with depth in the Moon; the confinement is frequency dependent and the shell within which the field is confined shrinks as the frequency is increased.

The topology of the idealized interplanetary magnetic field lines is given by Parker where the equation for the lines is that of an Archimedean spiral (Parker, 1963). This follows from a combination of the solar rotation period, the high electrical conductivity of the solar gas, and the assumption of constant outward velocity for the solar wind. The latter is substantially correct for most of the flow field because of the strongly supersonic flow. Components of the Parker field (in the ecliptic plane) are $B_r = B_{ro}(r_o/r)^2$ and $B_t = (\omega r/v_s)B_r$ where B_r is the component of the field radially outward from the Sun at r, B_{ro} is the radial component at the surface of the Sun, r_o is the solar radius, r the radius vector to the position of observation, B_t the tangential component, ω the angular velocity of the Sun, and v_s the bulk flow speed of the solar wind. The angle of the field measured between the outward pointing radius vector and the tangent to the field line at the position, r, is $\eta = \tan^{-1}(\omega r/v_s)$. Near Earth during quiet times, the ideal angle based upon v_s = 400 km/sec, is 45 deg. Thus the $\underline{k}$ vector field at the position of the Moon during quiet times is pointed at about 45 deg. away from the radius from the Sun. * During times of solar disturbance the field can take on any direction, and the spiral geometry is destroyed (Colburn and Sonett, 1966). Observation of induction by the solar wind field is limited to times when the Moon is in

Footnote

*Based upon Alfven waves propagating along the field lines.

the solar wind free of the magnetic tail of the Earth, though observation can be continued during those times when the Moon dwells in the post shocked plasma of the transition region behind the bow shock wave. The reason for the latter is that at lunar distance the post shocked plasma has returned nearly to the parameters found in the solar wind, and therefor the two are not easily distinguished.

It is our aim in the following sections to show the formal similarity between the problem of lunar electromagnetic induction and Mie scattering. For this demonstration we shall draw heavily upon earlier work. The key to the similarity lies in the applicable wave equations expressed in the next section which are seen to be just those of classical vacuum scattering of light from spherical objects. In the lunar case complications arise from the radial stratification of the conductivity function for the Moon, modification of the boundary conditions because of the pressure of the solar wind which results in the formation of a surface current layer (Blank and Sill, 1969; Schubert and Schwartz, 1969), and the existence, in principle, of steady state excitation corresponding to ohmic dissipation for the TM (transverse magnetic) mode which has no analog in vacuum scattering (Sonett and Colburn, 1967). Further for the Moon there is vanishingly small radiation field at least for frequencies considered here; the induced field is primarily due to magnetic multipole excitation and comprises only a near field. Electric multipoles are by no means ruled out but have so far not been detected. The dominance of magnetic excitation arises naturally from the large fulk electrical conductivity.

The basic equations written out in the next section have general applicability even for the more exact asymmetric induction problem which takes into account the existence of the lunar plasma cavity, but this paper is restricted to spherically symmetric induction. The two approaches are

not basically different, but asymmetric induction has been solved so far only for the low frequency limit (Schubert, et al., 1972). Modification of the mode spectrum by the introduction of higher frequencies is presently being worked out and the complete solution should be available at a later date.

FIELD EQUATIONS

The TE (transverse electric) and TM (transverse magnetic) wave equations are respectively

$$\nabla^2 \Omega^m + k^2 \Omega^m = 0 \tag{1}$$

and

$$\nabla^2 \Omega^e - \frac{1}{k_1 r} \frac{dk_1}{dr} \frac{\partial}{\partial r} \left(r \Omega^e \right) + k^2 \Omega^e = 0 \tag{2}$$

where equation 1 represents the transverse magnetic (TM) mode, equation 2 the transverse electric (TE) mode, $k^2 = \omega^2 \mu \epsilon + i \sigma \mu \omega$, $k_1 = i \omega \epsilon - \sigma$ and μ and ϵ are the magnetic permeability and electrical permittivity respectively. The field vectors E and H are determined from the potentials Ω^m and Ω^e. The potentials Ω^m and Ω^e are given by

$$\Omega^m = \mu V_s H_o \sin \phi \sum_{l=1}^{\infty} \beta_l A_l^m G_l^m (r) P_l^1 (\cos \theta) \tag{3}$$

and

$$\Omega^e = H_o \frac{a}{r} \cos \phi \sum_{l=1}^{\infty} \beta_l A_1^e G_1^e (r) P_l^1 (\cos \theta) \tag{4}$$

where v_s is the speed of the solar wind, a the lunar radius, r, θ, ϕ spherical polar coordinates, p_l^1 (cos θ) the associated Legendre

polynomials and

$$\beta_\ell = i^\ell \frac{(2\ell + 1)}{\ell(\ell + 1)}$$

The radial functions are solutions of the differential equations

$$\frac{d^2 G_\ell^m}{dr^2} + \left\{ k^2 - \frac{\ell(\ell + 1)}{r^2} \right\} G_\ell^m (r) = 0 \qquad (5)$$

and

$$\frac{d^2 G_\ell^e}{dr^2} - \frac{1}{k^2} \frac{d(k^2)}{dr} \frac{d G_1^e}{dr} + \left\{ k^2 - \frac{(\ell(1 + 1)}{r^2} \right\} G_\ell^e (r) = 0 \qquad (6)$$

A more complete theory of the induction has recently been given by Schubert, et al., (1972) which includes the asymmetry introduced by the flow field of the solar wind. However the fundamental properties of the induction can in most part be seen from the behavior of the spherically syymetric equations; departures are important but the latter theory is still under development for the time dependent case including the higher order time multipoles.

Induction in the Moon is expressed most conveniently by the formalism of Schubert and Schwartz (1969) where

$$\frac{H_s}{H_o} = \underset{\sim}{a}\, \underset{\sim}{y} + (\sigma_s \mu V_s R_m) \sin\gamma \cdot \underset{\sim}{\chi} \frac{\left\{ \frac{1}{2} + \frac{R_c^3}{R_m^3} + \frac{\sigma_s}{\sigma_c} \frac{p_1(k_c R_c)}{2 j_1(k_c R_c)} \left[1 - \frac{R_c^3}{R_m^3} \right] \right\}}{\left[1 - \frac{R_c^3}{R_m^3} + \frac{\sigma_s}{\sigma_c} \frac{p_1(k_c R_c)}{2 j_1(k_c R_c)} \left(2 + \frac{R_c^3}{R_m^3} \right) \right]}$$

$$- \frac{3}{2} \sin\alpha \cdot \underline{\alpha} \; \frac{\left(\frac{R_c}{R_m}\right)^3 \cdot B_1(k_c R_c)}{\left[1 - \left(\frac{R_c}{R_m}\right)^3 \cdot B_1(k_c R_c)\right]} \qquad (7)$$

for the magnetic field on the surface of the Moon. Here the first term represents the unit forcing field, the second the induction due to the TM mode and the last term that due to the TE mode. H_o is the forcing field, $\underline{a}_y$ a unit vector in the direction of H_o, $\underline{\chi}$ and $\underline{\alpha}$ unit vectors in the directions along the axis of toroidal symmetry and poloidal symmetry respectively, σ_s and σ_s are the shell and core conductivities for the model here of a two layer Moon, R_c and R_m the core and lunar radius respectively, μ the magnetic permitivity, v_s the solar wind speed, p_1 and j_1 are spherical Bessel functions in the notation of Stratton (Stratton, 1941) and B_1 is an induction number given by

$$B_1 (k_c R_c) = 1 - \frac{3}{k_c^2 R_c^2} + \frac{3 \cot(k_c R_c)}{k_c R_c} .$$

Lastly, γ and α are respectively the polar angles between the toroidal or poloidal axes to the position of observation on the surface of the Moon and k_c is the wave number in the core Equation (7) represents the lunar response for the lowest order induction, but higher orders are obtainable from the general formulae of Schubert and Schwartz (1969). For illustrative purposes the dipole order suffices, until later when higher order TE interaction is specifically addressed.

In equation (7) the second (TM) term is linearly dependent upon the speed of the solar wind, v_s, which determines the interplanetary electric field $\underline{E}_m = \underline{v}_s \times \underline{B}$ which drives the TM mode. However, experimental

findings show that this mode is suppressed and the lunar response is dominated by the TE mode as expected for a partially conducting material. We note that $B_1 < 1$ for all $k_c R_c$ and since $R_c < R_m$ the denominator can never vanish; however, large values for the ratio can be attained as $(R_c/R_m) B_1 \rightarrow 1$ confirming that a strong current layer exists on the sunward side of the Moon consistent with the dynamic pressure of the solar wind forcing into the Moon the induced magnetic field and yielding amplifications well in excess of those found for vacuum induction.

Although the customary treatment of scattering pays most attention to the far field, in the present case little radiation field is found. The near field dominates the response, and most attention is concentrated upon the interior of the scatterer, the Moon. We shall return to the properties of equation (7) in a later section.

THE GEOMETRY OF LUNAR INDUCTION AND THE RESPONSE (TRANSFER) FUNCTION

Viewed as a scattering problem the basic geometry of the excitation of lunar response by the solar wind electromagnetic field is shown in figure (1). $\underline{E}$, $\underline{B}$, and $\underline{k}$ are taken mutually orthogonally as is the case for Alfven waves propagating along the mean interplanetary magnetic field which is taken along $\underline{k}$ (not shown). For the case of Apollo 12 (from which the data shown in this paper are taken) the magnetometer lies nearly upon the lunar equator; the diagramatic representation of $\underline{k}$ in figure (1) is indicative of the mean geometry but time dependent deviations take place which are significant and must be accounted for. Such

details would not materially modify the present discussi on. The solar wind vector is shown as $\underline{V}_s$ making an angle δ with $\underline{k}$ and V_p (phase velocity). The position of the magnetometer (LSM) is also shown and θ is the scattering angle measured from the direction of $\underline{k}$ to the outward pointing radius vector from the center of the Moon to LSM. The response of the Moon for modal order higher than dipole is asymmetric and qualitatively indicated by the two functions A_θ and A_φ.

Data taken in the experiment discussed here are from the lunar satellite Explorer 35 which monitors the free stream solar wind magnetic field free of perturbing influences of the Moon, and the LSM which determined the surface field on the Moon.

Data taken in orbit are free of influence of the Moon because of the supersonic streaming of the solar wind which prevents upstream propagation of waves from the Moon.

We define an operational transfer function by

$$h_{2i}(f) + h_{1i}(f) = A(f)_i \cdot h_{1i}(f)$$

where $h_{2i}(f)$, $h_{1i}(f)$ are the Fourier transformed ith components of the forcing field and response field, f the frequency, and $A_i(f)$ the ith component of the transfer function, all defined in a rectangular coordinate system where x is vertical locally at the Lunar Surface Magnetometer (LSM) site, y locally eastward, and z northward. LSM measures the sum of the forcing field and the induction while Explorer 35 in lunar orbit measures only the former.

To give the reader some idea of the properties of the data obtained, figure (2) shows the transfer function as defined above. These data have been corrected for plasma noise on the lunar surface, and are

representative of the response in the frequency interval shown. As we shall see shortly the rollover at high frequency and of the scale is indicative of excitation of higher order magnetic multipoles. The transfer function attains values higher than 3 verifying that containment of field lines is taking place. The model Moons shown in the insert are best fit monotonic models. They are used to make the forward calculated curves shown superimposed upon the data, and correspond to different values of phase velocity which is explained subsequently (See Sonett, et al., 1972 for details).

PARTIAL WAVES

Equations (1) and (2) show that the partial wave excitation is practically restricted to the lowest order mode when the wavelength of the exciting radiation field is large compared to the scale size of the Moon, i.e., $\lambda \gg R_m$. This corresponds in the optical case to the Rayleigh limit. Actually for the Moon the problem is considerably more complex as higher order modes have been inferred in the iteration of the conductivity profile.

Assuming the idealized case of Alfven waves propagating along the direction of the mean solar wind magnetic field, $\underline{B}_o$, since $\underline{B}_o$ is spiralled because of the high conductivity of the plasma and the rotation of the Sun, the angle with respect to the radius vector from the Sun is about 45 degrees at 1 AU. Therefore the wave normals for the Alfven fields are slanted at about this angle. Since the angle of the mean field $\eta = \tan^{-1}(r/v_s)$ η changes depending upon the regional value of v_s. Other effects can also change the direction of $\underline{B}_o$ over more or less short periods of time. Furthermore the wave field is not necessarily purely

Alfevenic all the time, and the direction of the wave normals, $\underline{K}$, can vary. In general, however, a reasonable representation is obtained by the assumption of a mean field direction of about 45 deg.

Figures 3 and 4 show the partial fields for two cases calculated using the best three layer Moon conductivety profile. Figure 3 is for a scattering angle θ = 150 deg. and Figure 4 for θ = 120 deg. Both use a phase velocity, v_p = 200 km/sec. somewhat lower than the usually value, but not seriously in error. The total induced field is given by $\sum$, while the partial contributions are shown separated into real and quadrature parts. Both figures show significant increases in the higher order contributions as $2\pi r_m/\lambda$ increases, and the general conclusion that the Mie scattering range is attained is supported.

Although not a central issue in this paper we show in Figure 5 all the model conductivity functions determined by iterative techniques (Sonett, et al., 1972). These indicate generally the magnitude of the internal conductivity and justify the conclusion that displacement currents are ignorable generally in the Moon except perhaps near the surface. The various models give a concise statement of the limitation of uniqueness permitting various combinations of monotonic and current layers. All are electrically equivalent insofar as the amplitude of the induced field is considered, but differences in phase are likely. For the demonstrative purposes of this paper we use the best fit three layer (3L) model.

Variations in v_p and in scattering angle lead to different scattering amplitudes when the latter is calculated using the 3L model. Several cases are shown in Figure 6 for comparative purposes. The use of a small value of v_p shifts the wave-length spectrum to smaller values and therefore increase the contributions from the higher order modes as is seen by the steeper rollover. Cases calculated are for a scattering angle of θ = 150 degrees

which shows the rollover strongly. That the rollover is a strong function of scattering angle is seen by inspection of the upper part of the figure which uses a fixed value for v_p = 200 km/ sec. This clearly is an effect of mutual interference between the different multipoles of the scattered field.

WAVELENGTHS

So far we have shown that the wave equations for lunar scattering are identical to those for the generalized case of induction in a spherical object; it is necessary to show that the wavelength regime fits that required for Mie scattering. The wavelength of disturbances in the solar wind is inferred from the Fourier transformed of the time series record for each component of the magnetic field. This forcing field is measured on Explorer 35 lunar orbiter. Without knowledge of the solar wind speed it is impossible to infer the wavelength spectrum. Furthermore the wavelength is that taken normal to the surfaces of constant phase which generally are not oriented with $\underline{k}$ vector along the solar wind direction but along the spiral direction.

We assume a mean velocity for the solar wind, v_s, = 400 km/sec., which is the approximate observable mean value. Next the direction of the mean interplanetary field is determined using minimum variance techniques. This is based upon determining the total spectral variance for each of the three components of the field in an arbitrary coordinate system and then rotating until the direction of minimum variance is found. The mean field direction is also found using an averaging technique. Analysis shows the direction of minimum variance and mean field to be colinear; discussion is restricted to these cases and they form the basis for the comments made here.

Assumption of a reasonable solar wind speed and knowledge of the direction of the interplanetary magnetic and $\underline{k}$ fields permits a simple geometrical construction to be made to find the phase velocity and from

this the wavelength spectrum. Figure 7 shows a diagram of the geometry. The figure is a view down upon the plane of the ecliptic. The line OA is the radius vector from the Sun along which v_s is measured. (It is assumed that the solar wind is free of aberration, unimportant in the present context.) The line WW is the intersection of the ecliptic with the wave front; W_1W_1 is the wave front transported through the distance pp' by solar wind convection. (The propagation speed is small compared to this velocity.). The wavelength is defined by QP' so that a wave front is moved normal to itself in the time it takes for the wave front WW to convect through pp'. Therefore the phase velocity, $v_p = v_s \cos\theta$, and the wavelength is given by $\lambda = v_s \cos\theta / f$, where f is measured frequency. The wavelength regime for the frequencies encountered in the Apollo magnetometer experiment range from $7.7 \times 10^{-3} \leq S \leq 1.4$ measured in units of the scattering parameter $S = 2\pi R_m/\lambda$ where R_m is the lunar radius. Thus it is seen that the scattering range involved encompasses the Rayleigh limit at low frequency but extends well into the Mie regime at the high frequency end of the spectrum. The important consequence of this is the addition of higher order modes to the induction spectrum; the dominant magnetic multipole radiation of the excited field includes quadrupole, octupole and perhaps higher orders depending upon the forcing field configuration at the time of observation. Waves in the solar wind which are thought to be responsible for the bulk of the induction are consistent with Alfven waves propagating along the lines of force of the mean field. Such waves have been demonstrated by Belcher and Davis to be outward propagating and therefore "blue" shifted by the solar wind (Belcher and Davis, 1971). Their real frequencies are therefore likely still lower than those found by direct measurement in the frame comoving with the Moon. Such waves are known to be non-dispersive and have propagation speeds given by $V_a = B/(4\pi\rho)$

where B is the field intensity, and ρ the mass density of plasma. For typical solar wind conditions $V_a \simeq 50$ km/sec., and therefore the propagation speed can be ignored in a first order analysis when compared to the convection speed, V_s, of the solar wind.

SPECIAL PROPERTIES OF THE MOON, POLARIZATION, ETC.

This paper is restricted primarily to discussion of the electromagnetic excitation of the Moon by the Solar wind and formal similarity to Mie scattering. We have discussed the excitation of higher order modes and shown this to be consistent with magnetic type radiation, but a radiation field is likely to be vanishingly small. Thus the far field in the sense of radiation theory is important, and the principle response of the Moon which is detected by magnetometers consists of the near field which is non-radiative. The conditions are analogous to an antenna at very low frequency where radiation is trivially small and only the close-in non-radiating electromagnetic field is seen.

The Moon is a somewhat special object. Its high internal conductivity is consistent with the suppression of electric type excitation. As is well known such media are anamolously dispersive since the phase velocity increases with frequency. Displacement currents are ignored since $\sigma/\omega\epsilon \gg 1$, where σ is the bulk electrical conductivity, ω the angular frequency, and ϵ the inductive capacity (all units and definitions in the S. I. units). Actually near the surface of the Moon such currents are expected but cannot be large and probably are below detectability.

The TM mode can be shown by other arguments to probably be unimportant, at least so far as analysis of existing data so far undertaken can be used as a guide. As pointed out earlier in this paper, the TM mode has anomalous behavior because of the presence of the conducting solar wind which permits ohmic currents to flow in the steady state. This has no analogue in vacumn scattering. It can be shown that the ohmic currents must decrease monotonically as frequency is increased because skin depth effects come into play and force the lunar interior current streamlines nearer to the surface. Therefore the total resistance increases with an attendent decrease in the integrated current.

However the above argument cannot be correct for the reactive currents which flow in the TM mode. Using a simple two layer model for illustration, the capacity of the Moon can be shown to be the same as for a parallel plate

capacitor of the same surface area. However the effective plate separation depends upon the skin depth assumed which depends upon the frequency. The plate separation will decrease as the frequency is increased, so that the capacitive current will increase with frequency. Therefore a peak in the TM response can take place at some frequency which depends upon various factors such as the conductivity profile in the lunar interior.

Calculation suggests that these effects must be small; the absence of a detectible bow shock wave about the Moon shows that the steady state interaction is virtually suppressed. For these reasons present consideration of the Moon usually ignores the TM mode.

Polarization of signals from the Moon has not so far been detected, but theory indicates that the induced field should be elliptically polarized. The reason for the difficulty is that the incoming Alfven wave field carried in the solar wind appears, when tested, to have random polarization. Until sufficiently "clean" signals, i. e. swaths of data with linearly polarized waves having fixed polarization are found in the overall data set, it is difficult if not impossible to make an adequate polarization test of the induction. Difficulties also exist wi th the coherence between Explorer 35 and the lunar surface because a decoherence by the intervening solar wind. Nevertheless theoretical calculations show that the expected lunar echo at the high frequency end of the data should be elliptically polarized.

CAPTIONS

1. Geometry of the scattering process. The plane containing $\underline{E}$ and $\underline{B}$ is the plane of the disturbance wave in the solar wind. The propagation is shown along $\underline{k}$ which is also the direction of the interplanetary magnetic field for Alfven waves. V_s is the solar wind bulk velocity and $\underline{v}_p$ the phase velocity including the convection of the disturbance which dominates the actual propagation of waves in the solar wind. The position of the surface is indicated by LSM and the scattering angle, θ, is defined as the angle between $\underline{k}$ and the position vector of LSM referred to the center of the Moon. A_θ and A_φ are the response functions in the east-west and north-south directions; they are different for higher order modes.

2. Transfer function amplitude for lunar response corrected for plasma generated noise at the lunar surface. The insert shows best fit model conductivity profiles obtained by inversion of the transfer function together with an assumed value for phase velocity, v_p. Forward calculations of the lunar response are shown as the lines superimposed upon the data.

3. Partial wave contributions to the scattered (near) wave field showing the sum ($\sum$), and the real and imaginary parts of the partial waves for $1 \leq \ell \leq 5$ assuming v_p = 200 km/sec, and scattering angle θ = 150 deg.

4. Similar to Fig. 3 except for scattering angle θ = 120 deg.

5. Lunar internal conductivity profiles showing two layer (2L), three layer (3L), four layer (4L), core plus layer (CCL), current layer (CL), and double current layer (DCL) cases. All are approximately equivalent electrically, but significant differences do exist in the residual errors. Also no account has been taken of phase up to this time. For details see Sonett et al, (1972).

6. Forward calculation of transfer functions based upon the best fit three layer model of Fig. 5. The effects of varying v_p while holding θ fixed are shown in the lower part of the figure. All cases shown some rollover. The upper part of the figure demonstrates the effect of changing scattering angle while holding v_p fixed.

7. Geometry of plane waves propagating and convecting with the solar wind. The wave front WW moves one wavelength normal to itself in the time taken for the distance PP' tp be covered by solar wind convection. Thus wavelengths must be corrected downwards by the factor cos θ .

REFERENCES

Belcher, J. W. and Davis, L. 1971, Large Amplitude Alfven Waves in the Interplanetary Medium, 2. J. Geophys. Res. 76, 3534.

Blank, J. L. and Sill, W. R. 1969, Response of the Moon to the Time Varying Interplanetary Magnetic Field, J. Geophys. Res. 74, 736.

Colburn, D. S. and Sonett, C. P. 1966, Discontinuities in the Solar Wind, Space Science Reviews 5, 439.

Parker, E. N. 1963, Interplanetary Dynamical Processes, Interscience.

Schubert, G., and Schwartz, K. 1969, A Theory for the Interpretation of Lunar Surface Magnetometer Data. The Moon 1, 106.

Schubert, G., Sonett, C. P., Schwartz, K., and Lee, H. J. submitted, The Induced Magnetosphere of the Moon, J. Geophys. Res.

Schwartz, K. March, 1971, Interim Final Report, American Nucleonics, Corp.

Sonett, C. P. and Colburn, D. S. 1967, Establishment of a Lunar Unipolar Generator and Associated Shock and Wake by the Solar Wind, Nature 216, 340.

Sonett, C. P., Dyal, P., Parkin, C. W., Colburn, D. S., Mihalov, J. D., and Smith, B. F. 1971a, Whole Body Response of the Moon to Electromagnetic Induction by the Solar Wind. Science 172, 256.

Sonett, C. P., Smith, B. F., Colburn, D. S., Schubert, G. and Schwartz, K. 1972, The Induced Magnetic Field of the Moon: Conductivity Profiles and Inferred Temperature, Proc. 3rd Lunar Science Conf. Geochim. et Cosmochim. Acta, Suppl. 2, Vol. 3.

Stratton, J. A., 1941, Electromagnetic Theory, McGraw Hill.

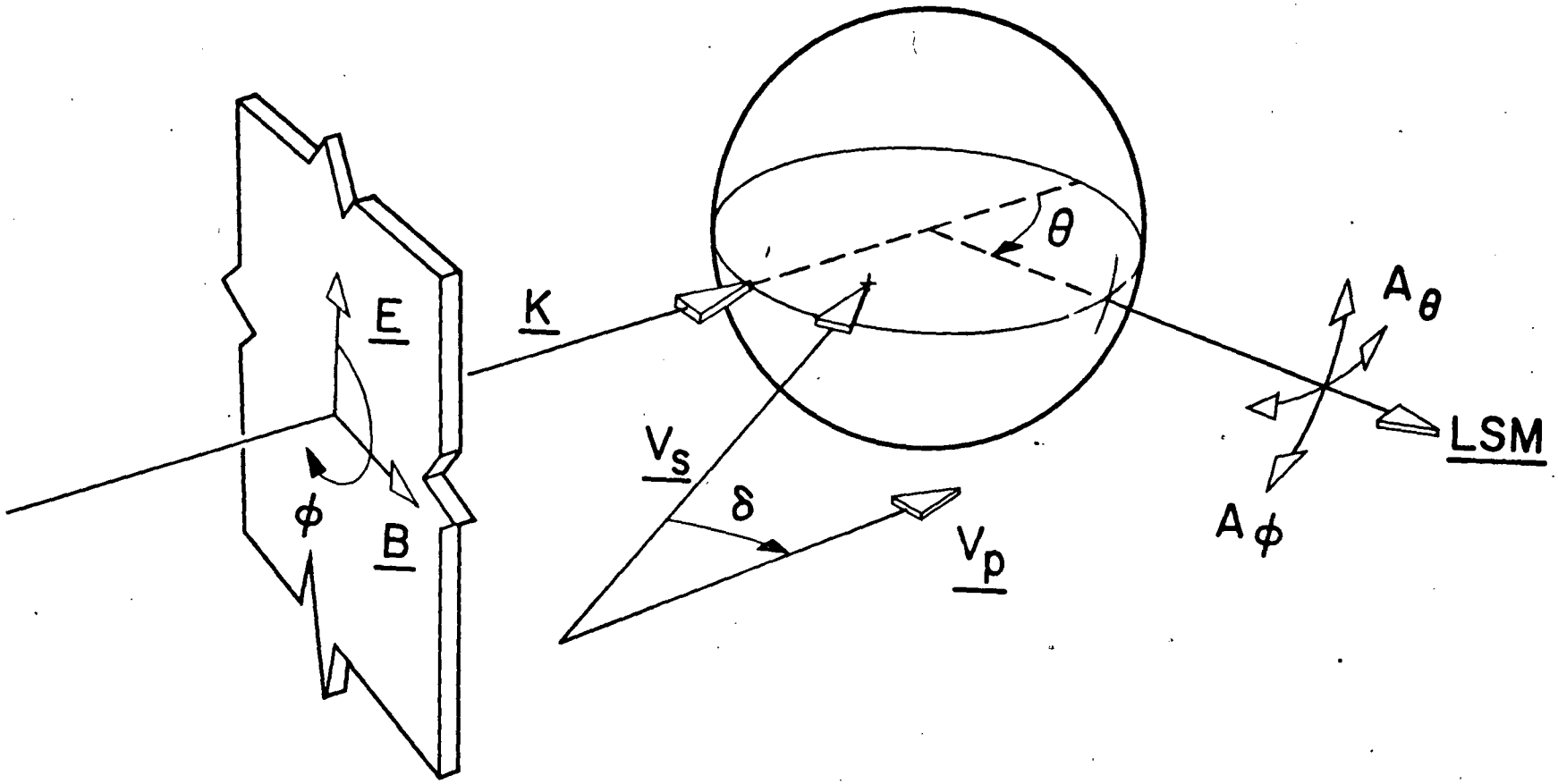

FIGURE 1

NATIONAL AERONAUTICS AND SPACE ADMINISTRATION
AMES RESEARCH CENTER; MOFFETT FIELD, CALIFORNIA

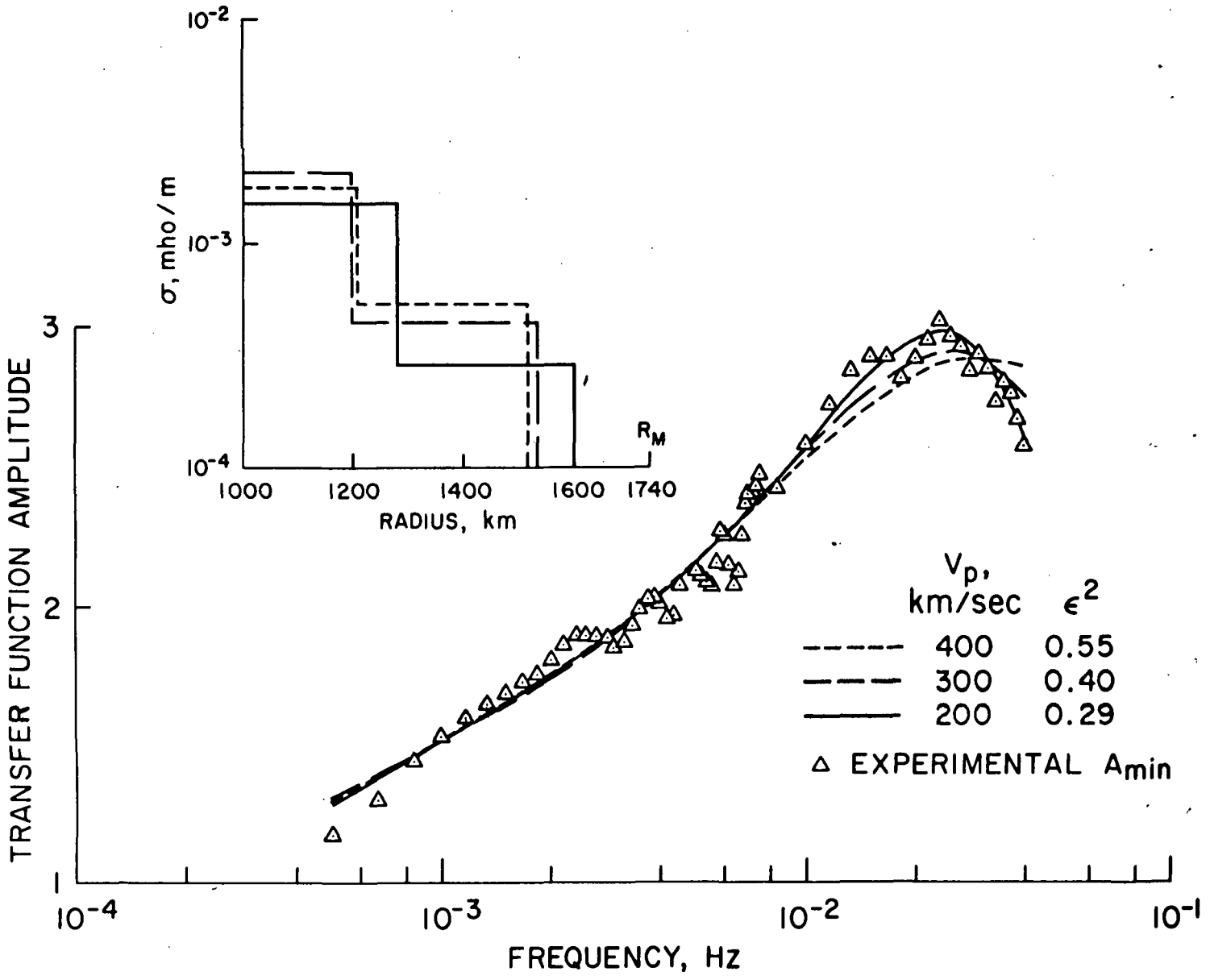

FIGURE 2

NATIONAL AERONAUTICS AND SPACE ADMINISTRATION
AMES RESEARCH CENTER, MOFFETT FIELD, CALIFORNIA

MULTIPOLE EXPANSION OF SCATTERED WAVE FIELD

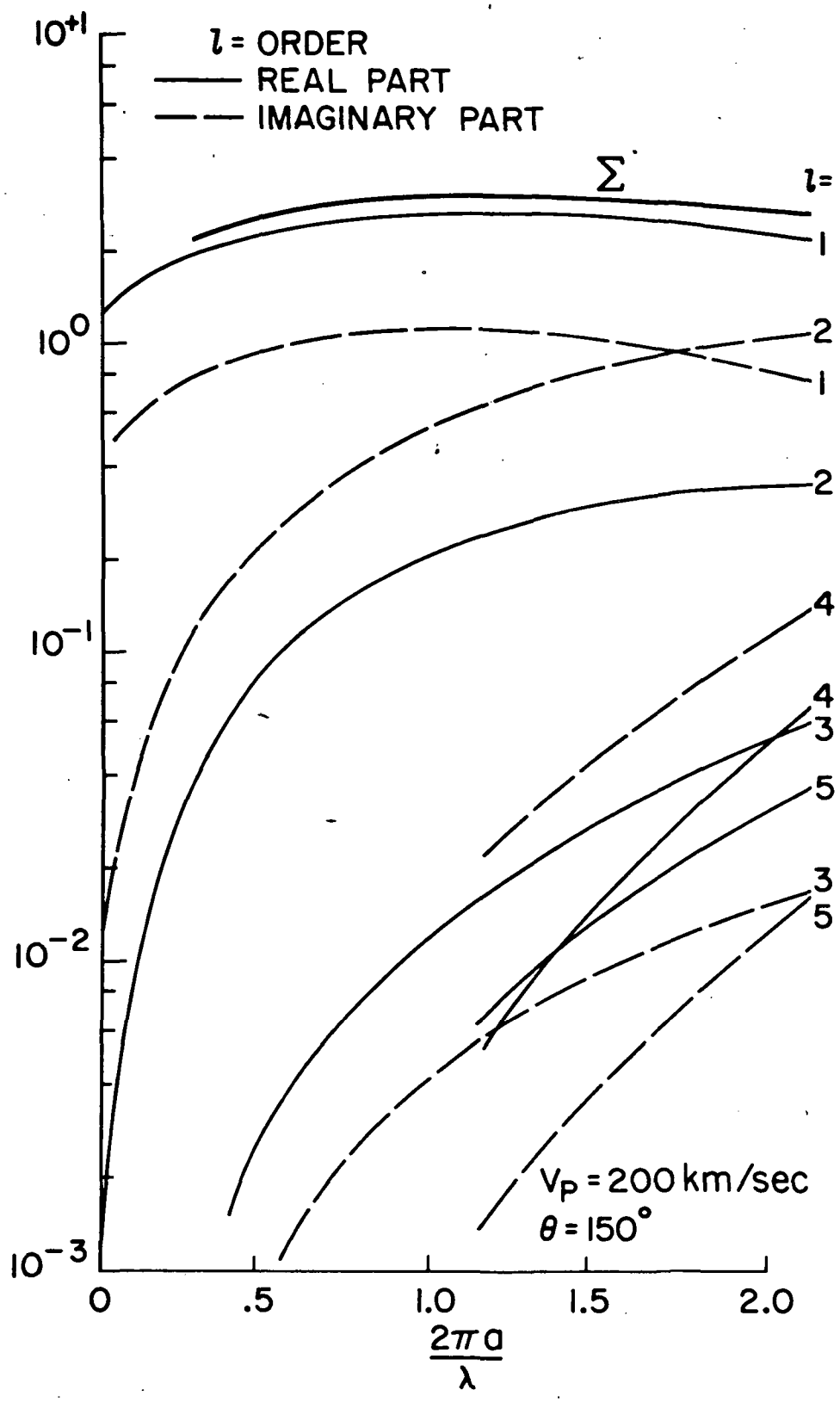

FIGURE 3

NATIONAL AERONAUTICS AND SPACE ADMINISTRATION
AMES RESEARCH CENTER, MOFFETT FIELD, CALIFORNIA

MULTIPOLE EXPANSION OF SCATTERED WAVE FIELD

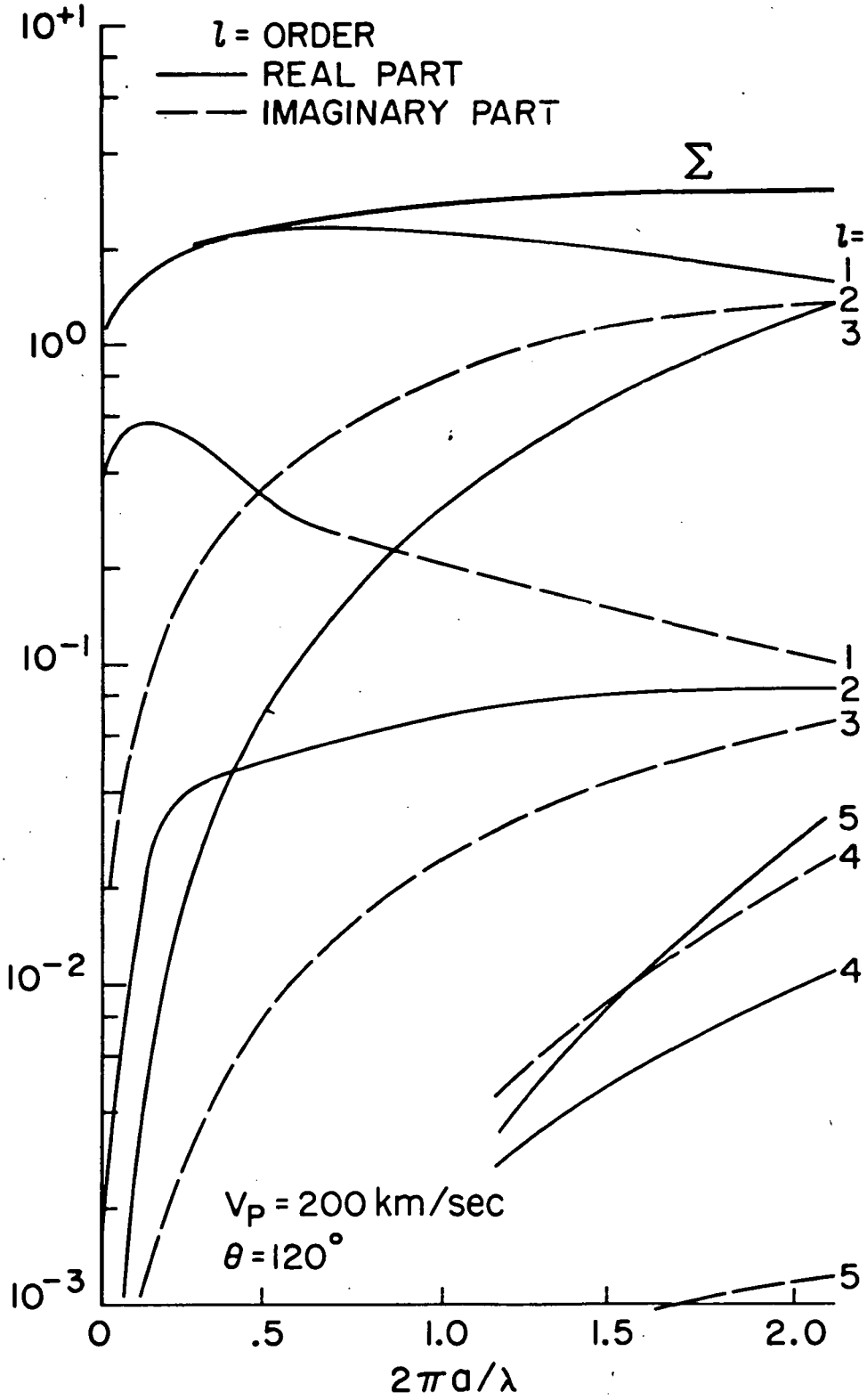

FIGURE 4

NATIONAL AERONAUTICS AND SPACE ADMINISTRATION
AMES RESEARCH CENTER, MOFFETT FIELD, CALIFORNIA

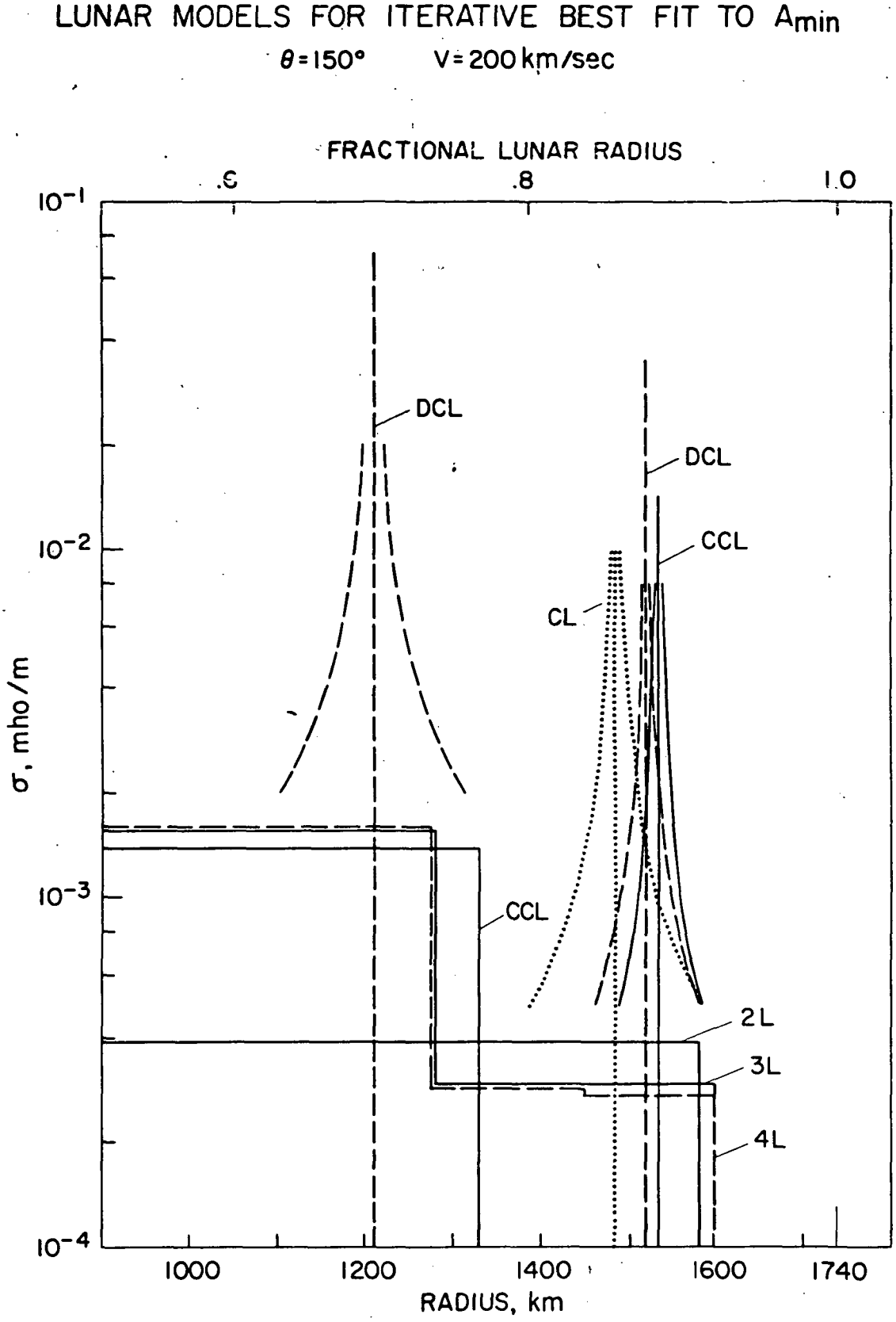
LUNAR MODELS FOR ITERATIVE BEST FIT TO Amin
θ=150° V=200 km/sec
FRACTIONAL LUNAR RADIUS
.6
.8
1.0
10⁻¹
10⁻²
10⁻³
10⁻⁴
σ, mho/m
DCL
DCL
CCL
CL
CCL
2L
3L
4L
1000
1200
1400
1600
1740
RADIUS, km

FIGURE 5

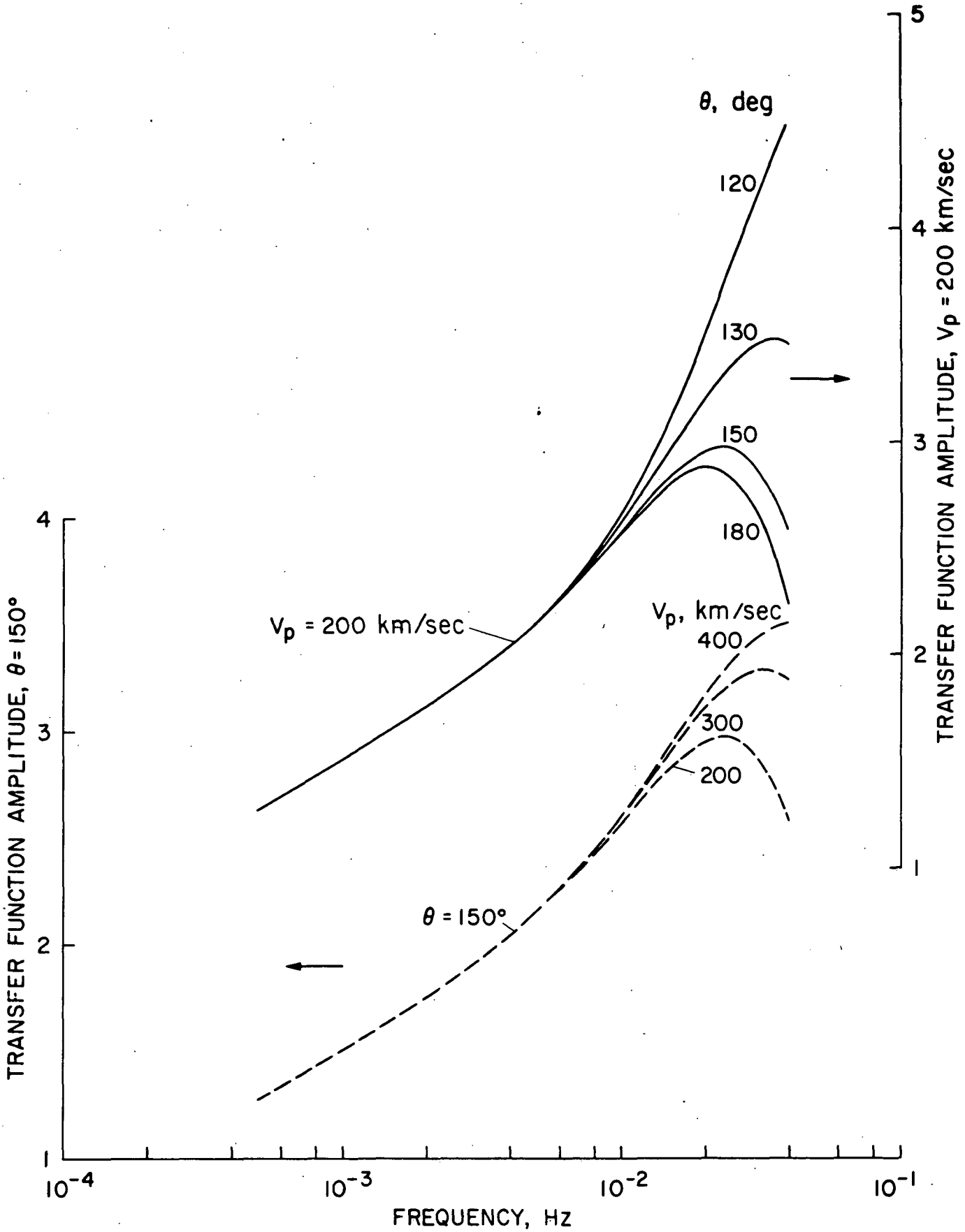
θ, deg
120
130
150
180
Vp = 200 km/sec
Vp, km/sec
400
300
200
θ = 150°
TRANSFER FUNCTION AMPLITUDE, θ = 150°
TRANSFER FUNCTION AMPLITUDE, Vp = 200 km/sec
FREQUENCY, Hz
1
2
3
4
5
10-4
10-3
10-2
10-1

FIGURE 6

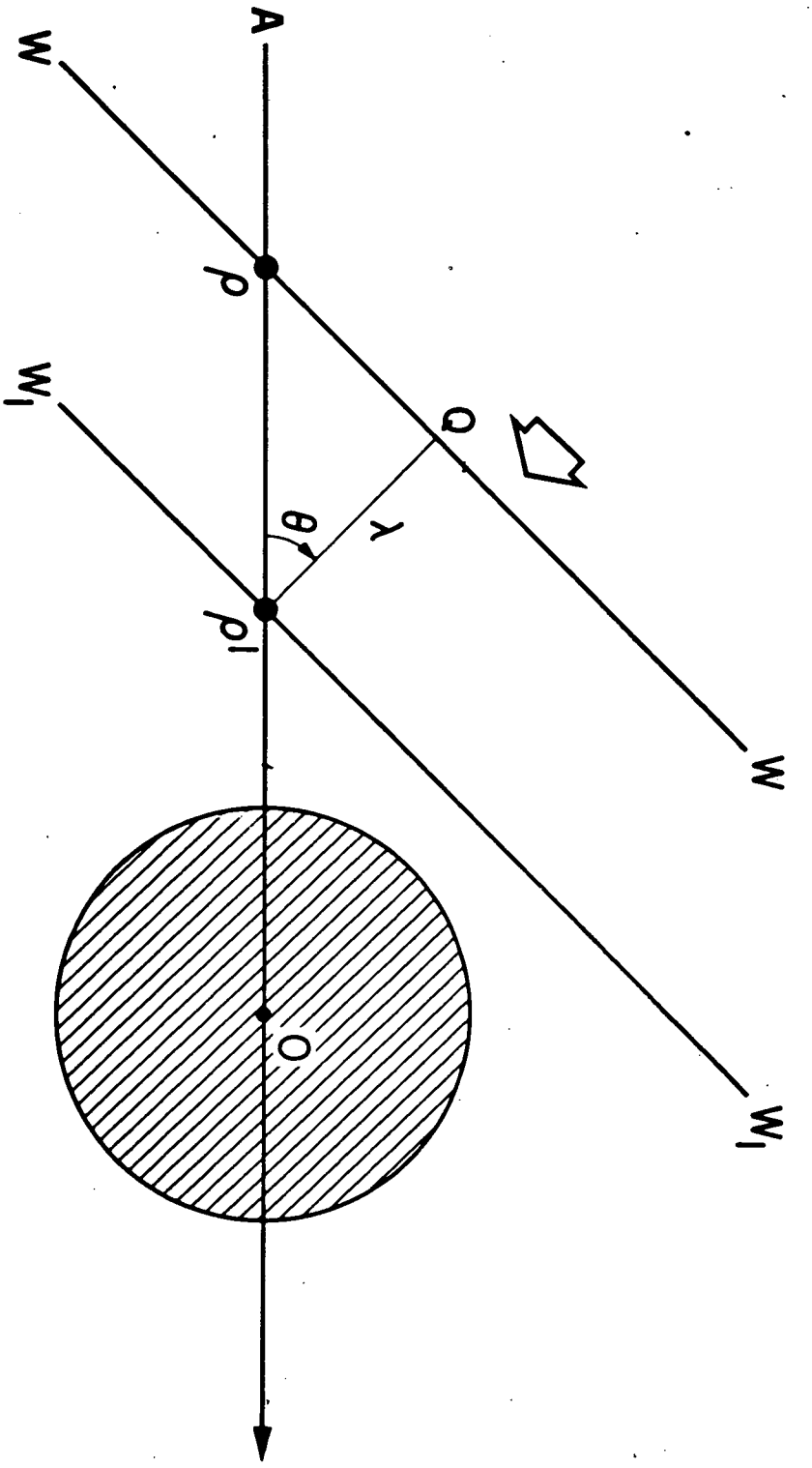

FIGURE 7